Mononuclear Lanthanide Complexes with 18-Crown-6 Ether: Synthesis, Characterization, Magnetic Properties and Theoretical Studies

Lindley Maxwell,[1,2] Martín Amoza,[1] Eliseo Ruiz*[1]

[1]*Departament de Química Inorgànica i Orgànica and Institut de Recerca de Química Teòrica i Computacional, Universitat de Barcelona, Diagonal 645, E-08028 Barcelona, Spain*

[2] *Advanced Lithium and Industrial Minerals Research Center, Universidad de Antofagasta, Av. Universidad de Antofagasta, 02800 Antofagasta, Chile*

e-mail: eliseo.ruiz@qi.ub.es

Abstract

A family of lanthanide metal complexes with general formula $[Ln(H_2O)_3(18\text{-crown-}6)](ClO_4)_3$ (Ln: Tb_{III}, Dy_{III}, Er_{III} and Yb_{III}) has been synthesized. Their magnetic properties have been characterized by DC and AC SQUID measurements and analyzed with the help of CASSCF-type calculations. The Dy_{III} and Yb_{III} compounds show slow relaxation of the magnetization under an external magnetic field. The analysis of the dependence of the relaxation time with the temperature and external magnetic field reveals that the main contributions are respectively the quantum tunneling and the Raman term, respectively. The analysis of the beta electron density and electrostatic potentials indicate that the axial ligands (three water molecules) generate a relatively small repulsion with the lanthanide electron density being the reason of the moderate magnetic anisotropy found in these systems.

INTRODUCTION

During last years, many research groups have made many different new molecular compounds using lanthanide atoms that behaves as single-molecule magnets (SMMs).[1-5] Recently, a breakthrough SMM behavior was detected in a dysprosium metallocene showing a blocking temperature of 60 K.[5] The main feature of this kind of compounds is to present a slow spin relaxation because the inversion of the spin is controlled by a relatively high energy barrier, 1760 K in the case of this dysprosocenium compound. However, there is not a unique parameter. Even higher barrier (1815 K) has been detected in a near-perfect pentagonal bipyramidal Dy_{III} compound but with a blocking temperature of 14 K.[6] There are different mechanisms that can provide the inversion of the spin: thermal jumping of the energy barrier through the spin-phonon interaction with the environment (Orbach mechanism), direct mechanism (coupling with one phonon), Raman mechanism (coupling with two phonons) and quantum tunneling in the ground or excited states. The slow relaxation mechanism is detected by two fingerprints: hysteresis loops showing steps due to the tunneling effects;[7] and the imaginary part of the magnetic susceptibility measured with AC magnetic fields presents a dependence with the frequency.[8] The latest is the usual employed approach because it does not required very low temperatures as the hysteresis measurements.

Since the paper of Ishikawa and coworkers published in 2003 presenting the first lanthanide mononuclear complex[9] (a Tb_{III} double decker showing slow spin relaxation) a large number of mononuclear lanthanide complexes exhibiting such behavior have been reported.[10-12] Among the lanthanide cations, the Dy_{III} systems are those showing more often single-molecule magnet behavior because they have a Kramers doublet ground state with a relatively high J value J = 15/2

and few electrons in the beta f shell that facilitates to adopt a more anisotropy shape of the electron density (in comparison with Er$_{III}$ also with Kramers doublet ground state with J=15/2). Despite such requirement, there are widely studied single-molecule magnets with integer J values with high-symmetric coordination modes as the phtalocyaninato Tb$_{III}$ systems mentioned above. It worth to mention that furthermore of the zero-field SMMs, many compounds exhibit slow relaxation of the magnetization under an external field.[13-16] Such magnetic field breaks the degeneracy of the up and down spin states by reducing the spin relaxation through quantum tunneling mechanism. Such systems are usually called *field-induced single-molecule magnets*, in contrast with those showing such behavior at zero field (*zero-field single-molecule magnets*).

Regarding the design of optimal mononuclear SMMs, a large number of crown ether complexes with lanthanides have been reported. Due to the cation size, the 18-crown-6 ether is the most adequate and a search in the Cambridge Structural database[17] gives 88 hits[18-60] being the most common lanthanides La$_{III}$, Eu$_{III}$, Nd$_{III}$, Ce$_{III}$ and Gd$_{III}$ with 18, 13, 12, 10 and 10 complexes, respectively. Among these compounds as it can be seen for the lanthanide cations, most of the described systems correspond to non-magnetic systems or light lanthanides. In the latest, slow magnetic relaxation was observed with Ce$_{III}$ and Nd$_{III}$ compounds.[61] Concerning the heavy lanthanides, they are expected to show larger magnetic anisotropy because J=L+S, instead of J=L-S for the early lanthanides. Despite this fact, the reported Tb$_{III}$ systems, for instance [Tb(18-crown-6)(NCS)$_3$] complex (CSD refcode WUHVUS) has not slow spin relaxation.[62] However, Ding and coworkers have characterized two Dy$_{III}$ complexes showing slow relaxation [Dy(18-crown-6)(NO$_3$)$_2$]X (X: ClO$_4$ and BPh$_4$) with energy barriers of 63 and 43 K, respectively.[63] It is worth to mention also that in some cases, the lanthanide cation remains out of a central cavity of the crown ether, resulting in a symmetrical "sandwich" if the metal is between two crown ethers while a non-symmetrical "sandwich" system is obtained when other ligands are coordinated to the metal.[64-65]

Here, the key point to have high magnetic anisotropy in such lanthanide complexes is that the spatial ligand distribution is able to accommodate the metal electron density in a localized region of the space with the minimal metal-ligand electron repulsion.[66-68] Some qualitative attempts have been made to establish basic criteria of how to reduce the electronic repulsion; thus, the analysis of the shape (prolate and oblate) of the ground-state electron density of the lanthanide cations together with the spatial distribution of the ligands proposed by Long and coworkers allows us to make useful predictions.[66] For instance, for the oblate Dy_{III} complexes, the disc shape electron density should be placed in a space region free of ligands (as for instance in the dysprosium complex) or with neutral ligands with relatively large metal-ligand distances in order to reduce the electrostatic repulsion. Thus, the electron density is concentrated in such region, adopting a non-distorted disc shape resulting in a highly anisotropy system with a very large perpendicular magnetic moment.

Taking into account the above ligand requirements, we have considered the use of the neutral 18-crown-6 to synthesize heavy lanthanide complexes that could be good candidates to have appealing magnetic properties. In this regard, computational methods based on CASSCF[69] calculations including spin-orbit effects are extremely helpful to understand the magnetic properties of this kind of complexes[70-78] because they can determine the relative importance of the different spin relaxation mechanisms (i.e, direct, tunneling, Raman and Orbach.[79]

EXPERIMENTAL SECTION

Synthesis of [Tb(H₂O)₃(18-crown-6)](ClO₄)₃ (1). $Tb(ClO_4)_3 \cdot 6H_2O$ (400 μl, 200 mg, 0.44 mmol) wt. 50 % in water were dissolved in 10 ml acetonitrile, and 10 ml of acetonitrile solution of 18-crown-ether (115 mg, 0.44 mmol) was added. The reaction was heated to 40 ℃ for 8 h. After slow evaporation of the filtrate over 3 days provided x-ray quality colorless crystals. The crystals were washed with diethyl ether to remove residues. The yield was 62 %. IR (cm-1) 3414, 1656, 1471,

1290, 1253, 1050, 950, 885, 838, 627. Caution! perchlorate salts of metal complexes with organic ligands are potentially explosive.

Synthesis of [Dy(H₂O)₃(18-crown-6)](ClO₄)₃ (2). $Dy(ClO_4)_3 \cdot 6H_2O$ (400 µl, 200 mg, 0.44 mmol) wt. 50 % in water was dissolved in 10 ml acetonitrile, and another 10 ml acetonitrile solution of 18-crown-ether (114 mg, 0.43 mmol) was added to it. The reaction was heated to 40 ₒC for 8 h. After cooling, the solution was filtered to remove insoluble substances and left to slow evaporate at room temperature. After few days a microcrystalline precipitate appeared. The crystalline materials and was dissolved in 5 ml of dry acetonitrile and after one week suitable colorless single crystals for X-ray crystallography were obtained. The crystals were washed with diethyl ether. The yield of product was 73 %. IR (cm₋₁) 3442, 2929, 1714, 1483, 1447, 1336, 1105, 1029, 978, 924, 875, 737, 698. Caution! perchlorate salts of metal complexes with organic ligands are potentially explosive.

Synthesis of [Er(H₂O)₃(18-crown-6)](ClO₄)₃ (3). $Er(ClO_4)_3 \cdot 6H_2O$ (400 µl, 200 mg, 0.43 mmol) wt. 50% in water was dissolved in 10 ml acetonitrile, and 10 ml acetonitrile solution of 18-crown-ether (114 mg, 0.43 mmol) was added to the first. The reaction was heated to 40°C for 8 h. After cooling, the solution was filtered. Clear, pink crystals were obtained *via* slow evaporation after 4 days. The crystals were washed with diethyl ether. The yield was 82 %. IR (cm₋₁) 3420, 2345, 1648, 1410, 1348, 1070, 965, 872, 833. Caution! perchlorate salts of metal complexes with organic ligands are potentially explosive.

Synthesis of [Yb(H₂O)₃(18-crown-6)](ClO₄)₃ (4). $Yb(ClO_4)_3 \cdot 6H_2O$ (400 µl, 200 mg, 0.43 mmol) wt. 50% in water was dissolved in 10 ml acetonitrile, where a 10 ml acetonitrile solution of 18-crown-ether (112 mg, 0.42 mmol) was added following a similar treatment as previous complexes. The reaction was heated to 40°C for 8 h. After cooling, the solution was filtered and left open at

5

room temperature. After 5 days colorless single crystals suitable for X-ray crystallography were obtained. The crystals were washed with diethyl ether (yield = 89 %). IR (cm^{-1}) 3418, 2350, 1641, 1403, 1352, 1067, 964, 875, 831. Caution! perchlorate salts of metal complexes with organic ligands are potentially explosive.

X-ray Crystallography. A Bruker D8 Venture (Mo Kα radiation, λ = 0.71073 Å, Photon 100 CMOS detector) diffractometer has been employed to measure single-crystals of **1**-**4**. Data collection, refinement parameters and crystal details are collected in Supporting Information (Table S1-S4). Once the data were processed (raw data integration, merging of equivalent reflections and empirical correction of the absorption), the structures were solved by either Patterson or Direct methods and refined by full-matrix least-squares on weighted F$_2$ values using the SHELX suite of programs.

Magnetic Measurements. Susceptibility measurements (Direct (DC) and alternating (AC) current) were carried out with a Quantum Design SQUID MPMS device. An oscillating *ac* field of 4 Oe were used in the Ac measurements and frequencies ranging from 1 to 1500 Hz and the external DC field indicated in the text. Polycrystalline species were mounted in a capillary tube made of polyimide. Samples of approximately 20 mg were not fixed within the sample tube and then they aligned along the magnetic field direction.

Computational Details. CASSCF method was used to calculated the state energies without spin-orbit effects for mononuclear complexes consisting of one Ln$_{III}$ cation surrounded by coordination sphere while the effect of spin–orbit coupling was taken into account perturbatively in a second step by using the restricted active space state interaction method (RASSI).[80] Dynamic correlation contributions are not essential due to the relative large ionic character of the Ln-O bonds. The MOLCAS ANO-RCC basis set[81-83] was used for all the atoms. The following contractions were

used: Tb, Dy, Er and Yb [9s8p6d4f3g2h]; O [4s3p1d]; N [4s3p1d]; S [4s3p1d]; F [3s2p]; C [3s2p] and H [2s]. (8,7), (9,7), (11,7) and (13,7) active spaces were used for Tb$_{III}$, Dy$_{III}$, Er$_{III}$ and Yb$_{III}$ systems respectively. For the Tb$_{III}$ system 7 septuplets and 140 quintuplets were used; for the Dy$_{III}$ system 21 sextets, 128 quadruplets and 98 doublets were used; for the Er$_{III}$ system 35 quadruplets and 112 doublets were used; finally, for the Yb$_{III}$ system 7 doublets were used. The direction and magnitude of the magnetic moment of the final states were evaluated using the SINGLE_ANISO routine implemented in MOLCAS 8.0.[71, 84] The matrix elements of the transition magnetic moments have been calculated to have an estimation about the probability of transition between two different states of the molecules.[85] Such matrix elements are calculated an integral between the two involved states, as it is proposed by the golden Fermi rule using a magnetic moment operator. DFT calculations were performed to obtain the electrostatic potentials of the ligand environment of the complexes using a model structure in which the metal atom is removed, using the B3LYP[86] functional with a TZVP basis set[87]using the Gaussian 09 package.[88]

RESULTS AND DISCUSSION

Crystal Structures of 1-4. The single-crystal X-ray diffraction of these four complexes (see Figure 1) were performed and the crystallographic data is reported in Table S1-S4. The crystal systems are quite different for this family of compounds: **1** is hexagonal, **2** orthorhombic while **3** and **4** are monoclinic. The molecules adopt different dispositions depending on the coordinated axial water molecules which, in addition, have several O-H⋯O hydrogen bonds with the perchlorate counteranions. Also, it is important to remark that this affects the packing causing changes in the crystal symmetries of the four crystals, where intermolecular interactions between the mononuclear lanthanide complexes are rather different. Thus, each Tb$_{III}$ compound (**1**) shows ten Tb⋯Tb intermolecular distances below 10 Å (2*8.482 Å, 2*9,752 Å, 6*9.857 Å) while the

other three complexes only six, being the Dy$_{III}$ compound the case with the longest intermolecular Ln···Ln contacts (1*8.548 Å, 1*8.587 Å, 2*8.934 Å, 2*9.985 Å). These differences are emphasized because intermolecular magnetic dipolar interactions are crucial for the spin relaxation through tunneling mechanism.[89]

1

2

3

4
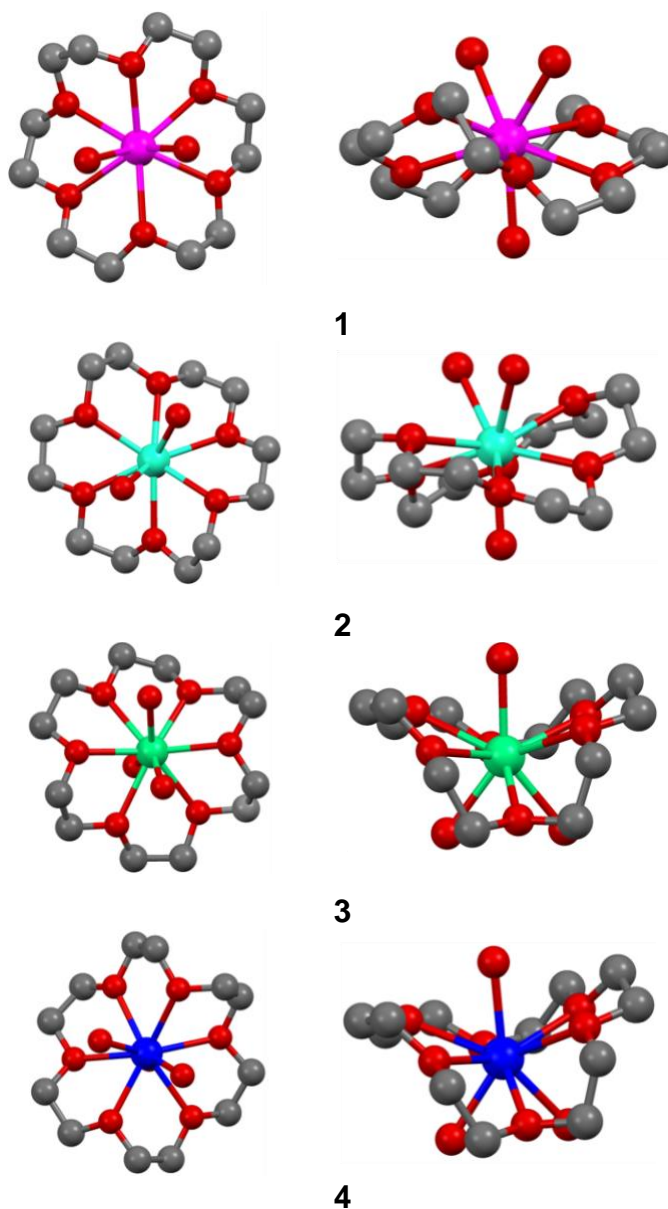
Figure 1 Two representations of the **1-4** lanthanide [Ln(H$_2$O)$_3$(18-crown-6)](ClO$_4$)$_3$ (Ln: Tb$_{III}$, Dy$_{III}$, Er$_{III}$ and Yb$_{III}$) complexes.

The use of the SHAPE code[90] allows the calculation of the coordination modes of the lanthanide cations. The lowest S values for the four systems (1.592, 1.561, 1.128 and 1.105, respectively for **1**-**4**) correspond to a muffin structure, this structure is relatively unusual, but it is adopted due to the slightly-distorted flat position of the six donor oxygen atoms of the crown ether.
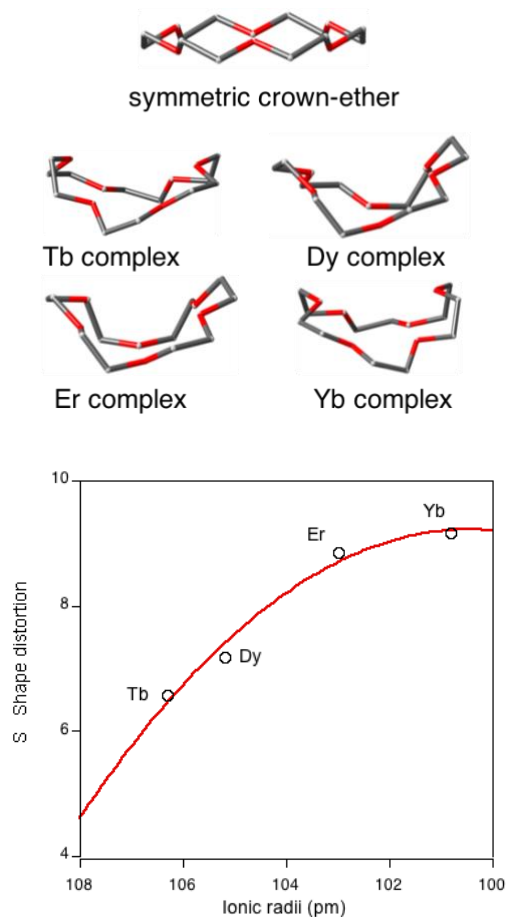

Figure 2 (top) Distortion of the crown-ether structure for the four lanthanide complexes **1**-**4**. (down) Representation of the crown-ether distortion estimated using the SHAPE program by comparing the position of the oxygen atoms with the hexagon of the symmetric crown-ether (lower S values higher symmetry).

To analyze the distortion of the crown-ethers due to the interaction with the lanthanide atoms, we have compared the adopted structure in the four systems with a symmetric crown-ether having a regular hexagonal disposition of the oxygen atoms (see Figure 2). The contraction of the heaviest lanthanide atoms results in a large distortion of the crown-ether to adopt the adequate structure to

9

interact with the metal. Furthermore, the analysis of the Ln-O bond distances (see Table S5) indicates that the complex with more similar bond distances is the Dy_{III} system indicating that such cation has the most appropriate size to fit inside the 18-crown-6 cavity to keep highest symmetry for the lanthanide complex. This compound also shows relatively large axial Dy-O bond distances with the water molecules (the average value is longer than Tb-O ones against the lanthanide contraction behavior, see Table S5). The analysis of the intermolecular hydrogen bond interactions shows that the shortest O···O distances, between the isolated axial water molecule (with the longest axial Dy-O distance) and the perchlorate counteranions, happen in the case of the Dy_{III} compound. Hence, for such system the enhancement of the intermolecular hydrogen bond interactions involving the axial water molecules could be the reason of the increase of the axial Dy-O distances.

Magnetic measurements. The thermal variation of the DC magnetic data (χ_MT vs. T plots) for complexes **1 – 4** (Figures S1-S4) shows χ_MT values at T = 300 K of 11.02 cm$_3$·K·mol$_{-1}$ (**1**), 13.01 cm$_3$·K·mol$_{-1}$ (**2**), 11.10 cm$_3$·K·mol$_{-1}$ (**3**) and 2.40 cm$_3$·K·mol$_{-1}$ (**4**) which are close to the theoretical value of 11.82, 14.17, 11.48 and 2.88 cm$_3$·K·mol$_{-1}$, respectively for each Ln_{III} ions in the free-ion approximation. The larger difference for Tb_{III} and Dy_{III} systems could be due to a more shorter intermolecular Ln-O-H···O-Cl-O···H-O-Ln exchange pathway than in the other two compounds. Upon cooling, the χ_MT products decrease continuously down to reach values of 6.0 cm$_3$ K mol$_{-1}$ (**1**), 7.7 cm$_3$ K mol$_{-1}$(**2**), 4.8 cm$_3$ K mol$_{-1}$ (**3**) and 1.48 cm$_3$ K mol$_{-1}$ (**4**) at 1.8 K. The *M vs H* plots (Figures S1-S4) at 1.8 K for complexes **1 – 4** show a rapid increase of the magnetization below 1 T and then a very slow linear increase to reach values of 4.7 *Nμ$_B$* (**1**), 4.9 *Nμ$_B$* (**2**), 4.3 *Nμ$_B$* (**3**) and 1.6 *Nμ$_B$* (**4**) at 5 T. These values are much lower than the expected saturation values (9.72, 10.65, 9.58 and 4.54 *Nμ$_B$*, respectively) and are compatible with the existence of strong crystal-field effects.

The analysis of AC magnetic susceptibility signal without an external applied static DC field indicates that no maximum in the χ'' signal was found for the four systems. Under a non-zero external field, Dy_{III} and Yb_{III} compounds show frequency-dependence with a maximum in the χ'' curves. Thus, when different small DC fields are applied, for instance 500 Oe in the case of Dy_{III} **2** compound (Figure 3a), the χ'' versus frequency signal at 1.8 K shows a maximum and a Cole-Cole diagram can be determined (Figure 3b).
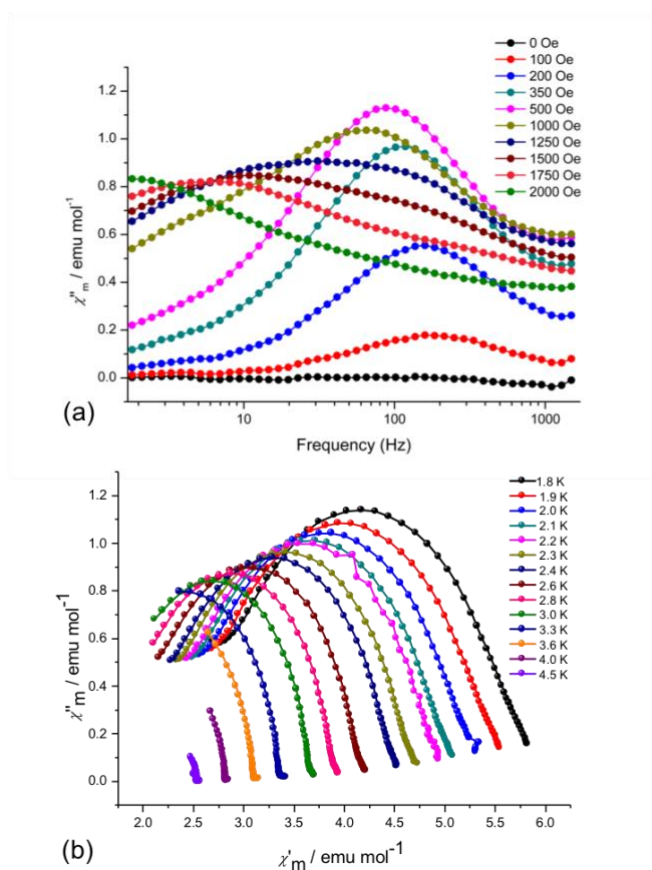
Figure 3 (a) Dependence for the [Dy(H$_2$O)$_3$(18-crown-6)](ClO$_4$)$_3$ complex of the out-of-phase susceptibility with the frequency at different static fields at 1.8 K. See Figure S5 for frequency dependence at different temperatures. (b) Cole-Cole diagram determined at 1.8 K and 500 Oe.

The Cole-Cole plots were fitted for the Dy_{III} compound and the relaxation times (see Figure 4) and α parameters calculated. The spin-lattice relaxation rate ♦ parameter was determined at each given temperature (see Table S6) that can be employed to analyze the spin relaxation mechanism by analyzing the ♦ vs. *T* dependence, following Equation 1:

$$t^{-1} = AH^4T + \frac{B_1}{1 + B_2 H^2} + CT^n + t_0^{-1}\exp\left(\frac{-U_{eff}}{kT}\right)$$

(1)

The terms in Equation 1 refer to direct relaxation, quantum tunneling, Raman and Orbach relaxation mechanisms, in that order.[79] Orbach processes are not considered because the *ab initio* calculations (see next section) indicate that the first excited state (46.6 cm-1) is much higher in energy than the determined with the last term of Equation 4 (12.9 cm-1) and the representation of ln ♦⌀⌂ vs. 1/T (not shown) does not present a clear linear dependence. Furthermore, the decrease of the ♦⌀⌂ values by increasing the external magnetic field (see Figure 4a) reveals that the direct term must be practically negligible. Thus, the spin relaxation is controlled by the quantum tunneling and Raman terms that can be used to fit the experimental data (red curves in Figures 4a and 4b). Recently, Ding and coworkers have proposed an approach to analyze the different relaxation processes for DyIII complexes.[91]

The Raman term has usually n values between 4 and 9 being important at higher temperatures. From the dependence with the temperature (Figure 4b) with the Raman term, we can extract $C=$ 0.432 s-1 K-8.23, $n = 8.23$ and $\tau_{QTM}^{-1} = 579$ s-1 (constant term added because quantum tunneling contribution has not temperature-dependence, Equation 2).

$$\tau^{-1} = \tau_{QTM}^{-1} + CT^n$$

(2)

Additionally, from the dependence with the field at 1.8 K (Figure 4a) it is possible to fit the experimental data with the $B_1 = 1089.2$ s-1, $B_2 = 426$ T-2 with a constant value that depends of the temperature $K(T) = 54.8$ s-1 (Equation 3) coming from the Raman term.

$$t^{-1} = \frac{B_1}{1 + B_2 H^2} + K(T)$$

(3)
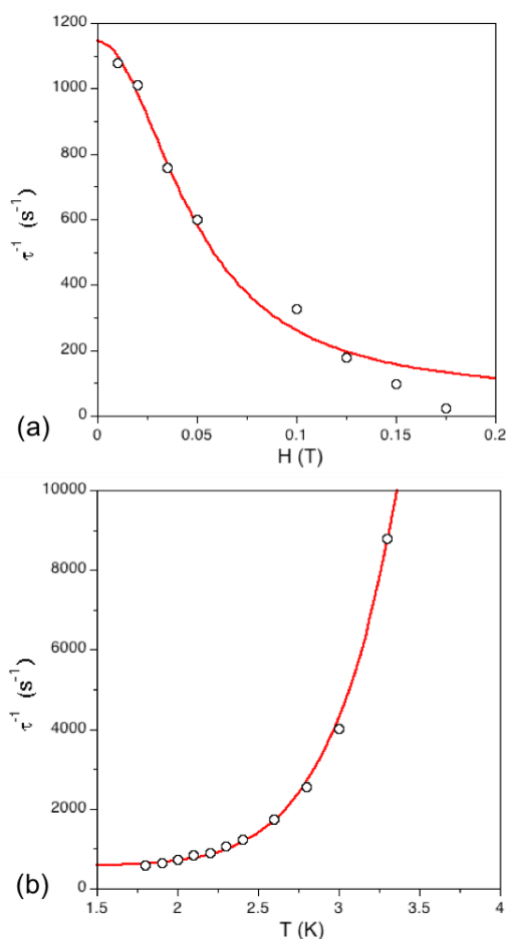
Figure 4 Dependence of the inverse of the spin relaxation time for the [Dy(H$_2$O)$_3$(18-crown-6)](ClO$_4$)$_3$ complex (a) with an static external field and (b) with the temperature. The red curves correspond to the fitting using the quantum tunneling (Equation 2) and Raman (Equation 3), respectively.

As mentioned above, also the Yb$_{III}$ compound shows a well-defined maximum in the χ'' signal (see Figure 5a) with an external field of 500 Oe. From the Cole-Cole diagram (Figure 5b) it is possible to extract the spin relaxation times by a fitting procedure (see Table S6 and Figure 6). In this case, despite to have only one unpaired electron, due to the 4f$_{13}$ configuration on the Yb$_{III}$ center, the Equation 1 must be applied due to the J = 7/2 value for its ground state. As in the case of the Dy$_{III}$ compound, the dependence with the external field is due to the quantum tunneling while the temperature-dependence is slightly different with two regions (above and below 2.5 K, see Figure 6a). Thus, it is expected that in the lowest temperature region, we have an Orbach

mechanism while at higher temperatures, due to the exponential dependence, the system follows a Raman mechanism. Again here, the Orbach term shows a fitted energy barrier from the experimental data (around 5 cm$_{-1}$) considerably smaller than the first excited energy determined with CASSCF calculations (63.3 cm$_{-1}$).
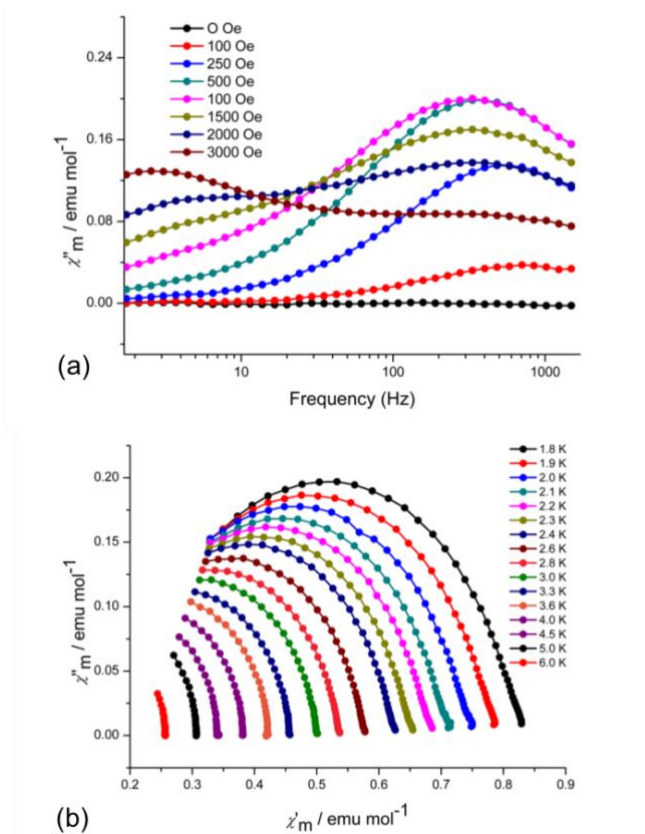
Figure 5 (a) Dependence for the [Yb(H$_2$O)$_3$(18-crown-6)](ClO$_4$)$_3$ complex of the out-of-phase susceptibility χ'' with the frequency at different static fields at 1.8 K. See Figure S6 for frequency dependence at different temperatures. (b) Cole-Cole diagram determined at 1.8 K and 500 Oe (down).

Due to the large number of parameters in the temperature dependence (by considering the Raman and Orbach) we fitted first the external field dependence, see Figure 6a, $B_1 = 3272.9$ s$_{-1}$ and $B_2 = 458.8$ s$_{-1}$T$_{-2}$ with $K(T) = 989.8$ s$_{-1}$. Then, for the temperature dependence we fitted first the low temperature region with an Orbach contribution. The fitted $\tau_{\square\square\square}$ and U_{eff} parameters were employed in the starting set of values for the full optimization (Orbach and Raman terms together)

with a small variation of such parameters.   The values found for the Orbach contribution are $\tau_{\square\text{ }D}$

$\square = 38339$ s-1 and $U_{eff} = 5.9$ K (4.1 cm-1) while for the Raman contribution from the temperature

dependence are $C = 0.3289$ s-1 K-5.80, $n=5.80$ and $\tau_{QTM}^{-1} = 1330$ s-1 (see Eq. 1).
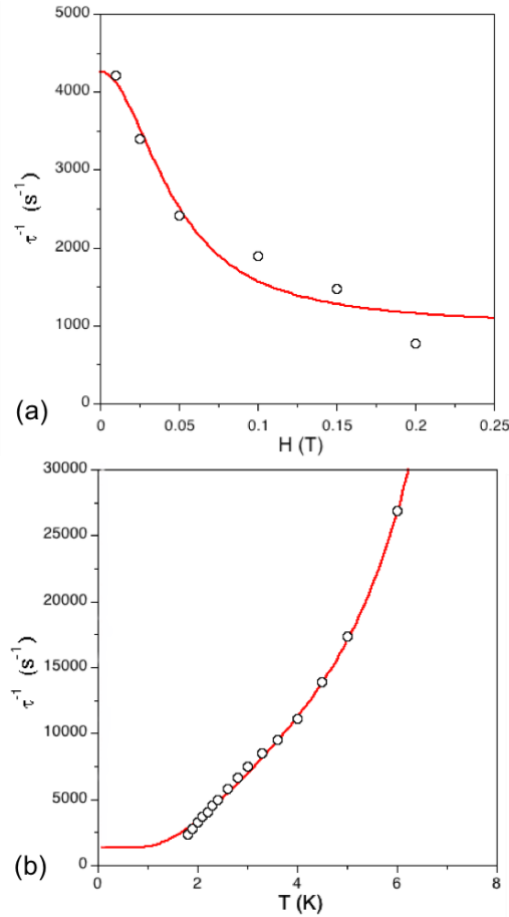
Figure 6 Dependence of the inverse of the spin relaxation time for the [Yb(H_2O)3(18-crown-6)](ClO4)3 complex (a) with an static external field and (b) with the temperature. The red curves correspond to the fitting using the quantum tunneling (Equation 2) and Raman (Equation 3), respectively.

The comparison of the fitted values for the DyIII and YbIII systems (see Table S6) allows the extraction of few interesting conclusions concerning the spin relaxation mechanisms: (i) The Raman exponent is smaller in the YbIII case, thus, at low temperature the Orbach mechanism cannot be neglected. (ii) From the spin relaxation time values, the relaxation is one order of magnitude slower in the case of the DyIII compound than for the YbIII one. (iii) Quantum tunneling mechanism is much more important in the case of YbIII as it is reflected in the larger B1 value. (iv) The two parameters of Raman term (C and n) are very different for both systems. C value for the YbIII compound is similar to that of the DyIII one, but the n value of DyIII is close to the

hypothetical limit of 9 while for Yb$_{III}$ compound is a value is close to 6. Hence, Raman mechanism is the dominating spin relaxation in the whole range of temperatures for the Dy$_{III}$ system while it is only at high temperatures for the Yb$_{III}$ one.

Multiconfigurational calculations. High-level calculations based on the CASSCF methodology by including spin-orbit effects with the RASSI approach (see Computational details section) have been employed to study the magnetic properties of the four synthesized compounds. From the analysis of the energy state distributions and the J values involved (see Figure 7 and Table S7), we can remark that the Tb$_{III}$ system is the unique case with an integer J value (J = 6), thus, the ground state is not a Kramers doublet. Despite that the first excitation energy is only 4.78 cm^{-1} (see Figure 7 and Table S7), this situation is not the most efficient to show large magnetic anisotropy because ground states with integer J values have stronger relaxation through quantum tunneling.[92]
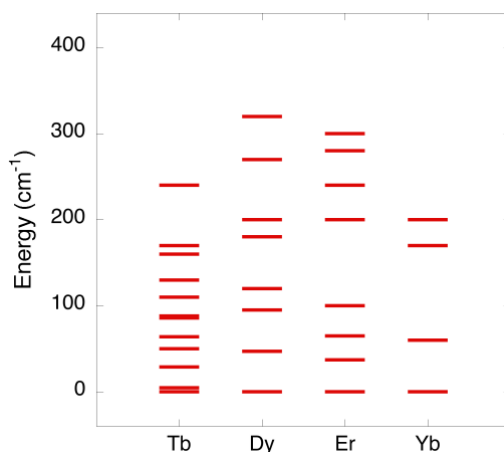
Figure 7 Energy distribution of the states including spin-orbit effects for the four studied complexes at CASSCF+RASSI level.

The Dy$_{III}$ and Er$_{III}$ systems have in principle the same J = 15/2 value and similar state energy distributions (see Figure 7). However, the Er$_{III}$ complex is less axial (g$_x$=1.87, g$_y$=3.33 and g$_z$=12.09) in comparison with the Dy$_{III}$ system (g$_x$=0.10, g$_y$=0.40 and g$_z$=18.51) and also has a very efficient spin relaxation mechanism through the quantum tunneling effect in the ground state (see Figure 8). Hence, such system does not display slow spin relaxation even under an external field.

In the case of the Yb$_{III}$ complex, the calculations show a relatively small axial character (g_x=0.23, g_y=2.38 and g_z=5.49). The larger quantum tunneling also found in the calculations (see green arrows in the ground state in Figure 8) agrees well with the much larger fitted B_l parameter from the experimental data; thus, the best SMM among these compounds is the Dy$_{III}$ system.
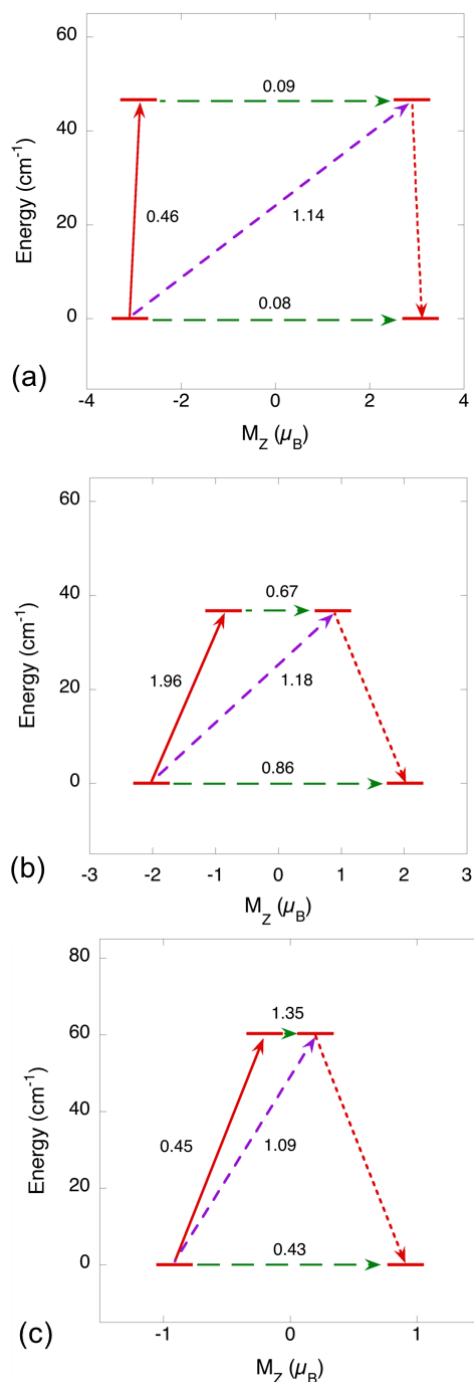

Figure 8 States energies as a function of their magnetic moment, M$_z$, along the main anisotropy axis for Dy$_{III}$ (a), Er$_{III}$ (b) and Yb$_{III}$ (c) systems. The green arrows correspond to the quantum

tunneling mechanism of ground and first excited states while purple arrow shows the hypothetical Orbach relaxation process. The red arrow indicates the transition between the ground and first Kramers doublets. The values close to the arrows indicate the matrix elements of the transition magnetic moments[85] (above 0.1 an efficient spin relaxation mechanism is expected, see Computational details).

In a previous paper,[68] we have analyzed the magnetic anisotropy of Dy_{III} complexes using the calculated CASSCF (spin-free) first and second excitation energies and the $(E_2-E_1)/E_1$ parameter. Such parameter can be considered as a figure of merit, thus, high values indicate large magnetic anisotropy. The calculated $(E_2-E_1)/E_1$ parameter for **2** is only 1.03 while values larger than 10 are expect for zero-field SMM; thus, the requirement of an external field to show slow spin relaxation is justified. The magnetic anisotropy in Dy_{III} complexes can be analyzed in terms of the oblate shape of the electron density expected for an axially-compressed shape equivalent to a disc ($_6H_{15/2}$ $m_J = 15/2$ ground state). This is closely related to the $(E_2-E_1)/E_1$ parameter, because the ground state and the first excited states have a similar disc-shape electron density while the second excited state has a different shape. Relatively large E_2 values are required to avoid the mixing with the second excited states when the spin-orbit effect is included, thus, the spin-orbit ground state will keep the disc-shape electron density, and consequently, it will show large magnetic anisotropy.

The electron density shape is basically controlled by the effect of the electrostatic potential of the ligands. In Fig. 9, the electrostatic potential generated by the ligands and the shape of the beta electron density (the alpha one is spherical) for **2** are plotted. The range of electrostatic potential values is very narrow, only 0.014 a.u., due to the presence of very similar oxygen donor atoms of the water molecules and from the crown-ether ligand. The potential is slightly more negative in the region with only one axial water ligand because the deformation of the crown-ether causes a concentration of donor oxygen atoms pointing towards such region. Thus, this lack of anisotropy in the electrostatic potential results in an isotropic electron density and the shape of the beta

electron density is considerably different of the oblate shape predicted for highly anisotropic Dy_{III} compounds. The presence of anions in the axial position would improve the magnetic anisotropy of such system. The beta electron densities for the other three lanthanide complexes are represented in Fig. S7.
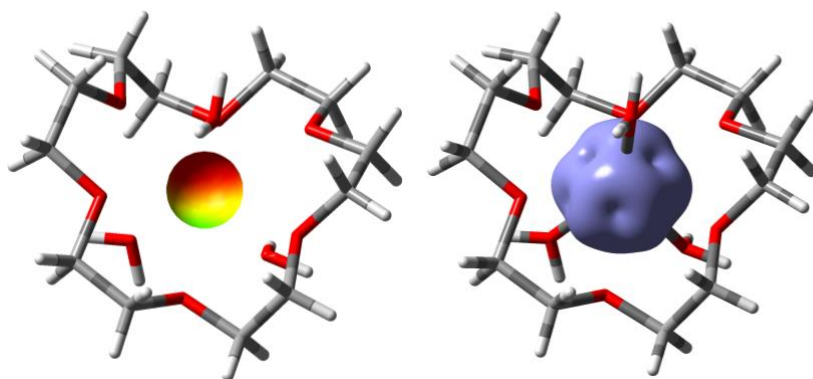
Figure 9 (left) Electrostatic potential projection (a range of 0.014 a.u. was adopted with the limit values in red and blue color, respectively, values) on a sphere of 1 Å of radius centered in the Dy position caused by the ligands fixed for the system **2**. (right) Isosurface of the calculated beta electron density of **2** calculated as the difference between the total density and the sum of the spin density of the seven alpha active electrons with the density of all doubly-occupied levels.

CONCLUSIONS

We reported the synthesis and characterization of a family of four lanthanide compounds with 18-crown-6 ether ligand and three axial water molecules. The crystal structures obtained using X-ray diffraction indicates a relatively large distortion of the 18-crown-6 ether ligand for the heavy lanthanide systems due to the lanthanide contraction. The study of dynamic magnetic properties reveals that the Tb_{III} and Er_{III} compounds do not show slow spin relaxation while the Dy_{III} and Yb_{III} complexes do, but in the presence of an external field. In the case of the Tb_{III} complex, such behavior is hindered by a non Kramers doublet ground state. The lack of perfect degeneracy in the

ground state difficults the existence of large magnetic anisotropy due to greater quantum tunneling contributions. However, in the Er$_{III}$ complex, CASSCF calculations indicate large g_x and g_y components that denote small axial character and a large quantum tunneling contribution. The magnetic properties of the Dy$_{III}$ and Yb$_{III}$ complexes were studied using squid AC measurements and theoretical CASSCF calculations. Both approaches show that the Dy$_{III}$ complex has a larger magnetic anisotropy, as expected for the larger J=15/2 ground state in comparison with J=7/2 for the Yb$_{III}$ system. The fitting of the relaxation time parameters with the external field can be performed using the quantum tunneling contribution, showing either experimental or theoretically a larger tunneling term for the Yb$_{III}$ system. Moreover, the dependence of the relaxation time with temperature is mostly reproduced through a Raman expression, however in the case of the Yb$_{III}$ system, the smaller exponent *n* of the Raman term (see Equation 2) makes that the Orbach mechanism is non-negligible at low temperatures. A deeper theoretical analysis was performed in the case of the Dy$_{III}$ system. The analysis of the calculated electrostatic potential created by the ligands and the shape of the electron density indicates that the similarities in the donor character between the oxygen atoms of the crown-ether and the water molecules results in an isotropic electrostatic potential around the metal where the electron density loses the anisotropic oblate character expected for an axial m$_J$=15/2 ground state. Thus, the inclusion of charge axial ligands would help to increase the magnetic anisotropy of such systems.

ACKNOWLEDGEMENTS

ASSOCIATED CONTENT

Supporting Information Available

Crystallographic Data and Structure Refinement of the four synthesized lanthanides systems (Tables S1-S4). Lanthanide-oxygen bond distances (Table S5). Static susceptibility and magnetization measurements for the four complexes (Figures S1-S4). Out-of-phase susceptibility χ'' dependence with the frequency for the $[Dy(H_2O)_3(18\text{-crown-}6)](ClO_4)_3$ and $[Yb(H_2O)_3(18\text{-crown-}6)](ClO_4)_3$ complexes (Figs. S5-S6). Spin relaxation time values for $[Dy(H_2O)_3(18\text{-crown-}6)](ClO_4)_3$ and $[Yb(H_2O)_3(18\text{-crown-}6)](ClO_4)_3$ complexes (Table S6). CASSCF+RASSI energies for the four studied systems (Table S7). Draws of the beta electron density for **1**, **3** and **4** complexes. This information is available free of charge via the Internet at http://pubs.acs.org.

Accession Codes

CCDC 1850168-1850171 contain the supplementary crystallographic data for this paper. These data can be obtained free of charge via www.ccdc.cam.ac.uk/data_request/cif, or by emailing data_request@ccdc.cam.ac.uk, or by contacting The Cambridge Crystallographic Data Centre, 12 Union Road, Cambridge CB 1EZ, UK; fax: +44 1223 336033.

REFERENCES

1. Woodruff, D. N.; Winpenny, R. E. P.; Layfield, R. A., Lanthanide Single-Molecule Magnets. *Chem. Rev.* **2013**, *113*, 5110-5148.
2. Zhang, P.; Guo, Y.-N.; Tang, K., Recent advances in dysprosium-based single-molecule magnets: Structural overview and synthetic strategies. *Coord. Chem. Rev.* **2013**, *11-12*, 1728-1763.
3. Luzon, J.; Sessoli, R., Lanthanides in molecular magnetism: so fascinating, so challenging. *Dalton Trans.* **2012**, *41*, 13556-13556.

4. Menelaou, M.; Ouharrou, F.; Rodríguez, L.; Roubeau, O.; Teat, S. J.; Aliaga-Alcalde, N., Dy[III]- and Yb[III]-Curcuminoid Compounds: Original Fluorescent Single-Ion Magnet and Magnetic Near-IR Luminescent Species. *Chem. Eur. J.* **2012**, *18*, 11545-11549.

5. Goodwin, C. A. P.; Ortu, F.; Reta, D.; Chilton, N. F.; Mills, D. P. Molecular magnetic hysteresis at 60 kelvin in dysprosocenium. *Nature* **2017**, *548*, 439-442.

6. Ding, Y.-S..;Chilton, N. R.; Winpenny, R. E. P., Zheng, Y.-Z., On Approaching the Limit of Molecular Magnetic Anisotrpy: A Near-Perfect Pentagonal Bypyramidal Dysprosium(III) Single-Molecule Magnet. *Angew. Chem. Int. Ed.* **2016**, *55*, 16071-16074.

7. Friedman, J. R.; Sarachik, M. P.; Ziolo, R., Macroscopic Measurement of Resonant Magnetization Tunneling in High-Spin Molecules. *Phys. Rev. Lett.* **1996**, *76*, 3830-3833.

8. Langley, S. K.; Chilton, N. F.; Moubaraki, B.; Murray, K. S., Anisotropy barrier enhancement via ligand substitution in tetranuclear {Co[III]2Ln[III]2} single molecule magnets. *Chem. Commun.* **2013**, *49*, 6965-6965.

9. Ishikawa, N.; Sugita, M.; Ishikawa, T.; Koshihara, S. Y.; Kaizu, Y., Lanthanide double-decker complexes functioning as magnets at the single-molecular level. *J. Am. Chem. Soc.* **2003**, *125*, 8694-8695.

10. Gao, F.; Cui, L.; Song, Y.; Li, Y.-Z.; Zuo, J.-L., Calix[4]arene-Supported Mononuclear Lanthanide Single-Molecule Magnet. *Inorg. Chem.* **2014**, *53*, 562-567.

11. Liu, J.; Chen, Y.-C.; Liu, J.-L.; Vieru, V.; Ungur, L.; Jia, J.-H.; Chibotaru, L. F.; Lan, Y.; Wernsdorfer, W.; Gao, S.; Chen, X.-M.; Tong, M.-L., A Stable Pentagonal Bipyramidal Dy(III) Single-Ion Magnet with a Record Magnetization Reversal Barrier over 1000 K. *J. Am. Chem. Soc.* **2016**, *138*, 5441-5450.

12. Zhang, P.; Zhang, L.; Wang, C.; Xue, S.; Lin, S.-Y.; Tang, J., Equatorially Coordinated Lanthanide Single Ion Magnets. *J. Am. Chem. Soc.* **2014**, *136*, 4484-4487.

13. Casanovas, B.; Font-Bardía, M.; Speed, S.; El Fallah, M. S.; Vicente, R., Field-Induced SMM and Visible/NIR-Luminescence Behaviour of Dinuclear Ln[III] Complexes with 2-Fluorobenzoate. *Eur. J. Inorg. Chem.* **2018**, *2018*, 1928-1937.

14. Qiao, S.; Zhang, J.; Zhang, S.; Yang, Q.; Wei, Q.; Yang, D.; Chen, S., Field-induced single-molecule magnet (SMM) behavior of dinuclear Dy[III] system. *Inorg. Chim. Acta* **2018**, *469*, 57-65.

15. Smolko, L.; Černák, J.; Kuchár, J.; Rajnák, C.; Titiš, J.; Boča, R., Field-Induced Slow Magnetic Relaxation in Mononuclear Tetracoordinate Cobalt(II) Complexes Containing a Neocuproine Ligand. *Eur. J. Inorg. Chem.* **2017**, *2017*, 3080-3086.

16. Xiang, J.; Liu, J.-J.; Chen, X.-X.; Jia, L.-H.; Yu, F.; Wang, B.-W.; Gao, S.; Lau, T.-C., Slow magnetic relaxation in a mononuclear 8-coordinate Fe(II) complex. *Chem. Commun.* **2017**, *53*, 1474-1477.

17. Allen, F. H., The Cambridge Structural Database: A quarter of a million crystal structures and rising. *Acta Crystallogr. Sect. B: Struct. Sci.* **2002**, *58*, 380-388.

18. Arliguie, T. r. s.; Belkhiri, L.; Bouaoud, S.-E.; Thuéry, P.; Villiers, C.; Boucekkine, A.; Ephritikhine, M., Lanthanide(III) and Actinide(III) Complexes [M(BH4)2(THF)5][BPh4] and [M(BH4)2(18-crown-6)][BPh4] (M = Nd, Ce, U): Synthesis, Crystal Structure, and Density Functional Theory Investigation of the Covalent Contribution to Metal-Borohydride Bonding. *Inorg. Chem.* **2009**, *48*, 221-230.

19. Arndt, S.; Spaniol, T. P.; Okuda, J., The first structurally characterized cationic lanthanide–alkyl complexes *Chem. Commun.* **2002**, 896-897.

20. Atwood, J. L.; Barbour, L. J.; Dalgarno, S.; Raston, C. L.; Webb, H. R., Supramolecular assemblies of p-sulfonatocalix[4]arene with aquated trivalent lanthanide ions. *J. Chem. Soc., Dalton Trans.* **2002**, 4351-4356.

21. Backer-Dirks, J. D. J.; Cooke, J. E.; Galas, A. M. R.; Ghotra, J. S.; Gray, C. J.; Hart, F. A.; Hursthouse, M. B., Complexes of lanthanide ions with the crown ether 1,4,7,10,13,16-hexaoxacyclo-octadecane. *J. Chem. Soc., Dalton Trans.* **1980**, 2191-2191.

22. Bakker, J. M.; Deacon, G. B.; Junk, P. C., Rare earth thiocyanate complexes with 18-crown-6 co-ligands. *Polyhedron* **2013**, *52*, 560-564.

23. Benetollo, F.; Bombieri, G.; De Paoli, G., *Eur. Cryst. Meeting* **1979**, *5*, 206-206.

24. Bombieri, G.; de Paoli, G.; Benetollo, F.; Cassol, A., Crown ether complexes of lanthanoid and actinoid elements. Crystal and molecular structure of $Nd(NO_3)_3$(18-crown-6). *J. Inorg. Nucl. Chem.* **1980**, *42*, 1417-1422.

25. Bünzli, J.-C. G.; Klein, B.; Wessner, D., Crystal and molecular structure of the 1:1 complex of 18-crown-6 ether with neodymium nitrate. *Inorg. Chim. Acta* **1980**, *44*, L147-L149.

26. Bünzli, J.-C. G.; Klein, B.; Wessner, D.; J. Schenk, K.; Chapuis, G.; Bombieri, G.; De Paoli, G., Crystal and molecular structure of the 4:3 complex of 18-crown-6 ether with neodymium nitrate. *Inorg. Chim. Acta* **1981**, *54*, L43-L46.

27. Champion, M. J. D.; Farina, P.; Levason, W.; Reid, G., Trivalent scandium, yttrium and lanthanide complexes with thia-oxa and selena-oxa macrocycles and crown ether coordination. *Dalton Trans.* **2013**, *42*, 13179-13179.

28. Chen, J.; Zhang, Y.-F.; Zheng, X.; Vij, A.; Wingate, D.; Meng, D.; White, K.; Kirchmeier, R. L.; Shreeve, J. n. M., Synthesis of Cyclic Ethers with Fluorinated Side Chains. *Inorg. Chem.* **1996**, *35*, 1590-1601.

29. Chesman, A. S. R.; Turner, D. R.; Deacon, G. B.; Batten, S. R., New Approaches to 12-Coordination: Structural Consequences of Steric Stress, Lanthanoid Contraction and Hydrogen Bonding. *Eur. J. Inorg. Chem.* **2010**, *2010*, 2798-2812.

30. Dalgarno, S. J.; Hardie, M. J.; Makha, M.; Raston, C. L., Controlling the Conformation and Interplay of p-Sulfonatocalix[6]arene as Lanthanide Crown Ether Complexes. *Chem. Eur. J.* **2003**, *9*, 2834-2839.

31. Drljaca, A.; Hardie, M. J.; Raston, C. L.; Webb, H. R.; Johnson, J. A., Lanthanum(III) capture of 18-crown-6 in the cavity of p-sulfonatocalix[4]arene. *Chem. Commun.* **1999**, 1135-1136.

32. Forsellini, E.; Benetollo, F.; Bombieri, G.; Cassol, A.; De Paoli, G., ChemInform Abstract: Preparation, Crystal And Molecular Structure Of $GdCl_3$(18-crown-6).EtOH *Chemischer Informationsdienst* **1985**, *16*.

33. Forsellini, E.; Benetollo, F.; Bombieri, G.; Cassol, A.; De Paoli, G., Preparation, crystal and molecular structure of $GdCl_3$(18-crown-6)·EtOH. *Inorg. Chim. Acta* **1985**, *109*, 167-171.

34. Harman, M. E.; Hart, F. A.; Hursthouse, M. B.; Moss, G. P.; Raithby, P. R., 12-Coordinated crown ether complex of lanthanum; X-ray crystal structure. *J. Chem. Soc., Chem. Commun.* **1976**, 396-396.

35. Hassaballa, H.; Steed, J. W.; Junk, P. C.; Elsegood, M. R. J., Formation of Lanthanide and Actinide Oxonium Ion Complexes with Crown Ethers from a Liquid Clathrate Medium. *Inorg. Chem.* **1998**, *37*, 4666-4671.

36. Hitchcock, P. B.; Khvostov, A. V.; Lappert, M. F.; Protchenko, A. V., Ytterbium(II) amides and crown ethers: addition versus amide substitution. *J. Organ. Chem.* **2002,** *647*, 198-204.

37. Hitchcock, P. B.; Lappert, M. F.; Layh, M., Novel lithium 3-sila- and 3-germa-β-diketiminates. *Chem. Commun.* **1998**, 2179-2180.

38. Hursthouse, M. B.; Arif, M. A.; Hart, F. A., *CSD Communication (Private Communication)* **2003**.

39. Jingwen, Y.; Baosheng, L.; Jingqiu, W.; Shaohui, Z., No Title. *Gaodeng Xuexiao Huaxue (Chem. J. Chin. Univ.(Chinese Edition))* **1987**, *8*, 559-559.

40. Koner, R.; Nayak, M.; FergusonPermanent address: Departme, G.; Low, J. N.; Glidewell, C.; Misra, P.; Mohanta, S., Strongly hydrogen bonded interlocked infinite double helices in a

crown ether based gadolinium(III) hexacyanoferrate(III) supramolecule. *CrystEngComm* **2005**, *7*, 129-129.

41. Mao, J.-G.; Jin, Z.-S.; Ni, J.-Z., *Jiegou Huaxue(Chin.)(Chin. J. Struct. Chem.)* **1994**, *13*, 377-377.

42. Misra, P.; Koner, R.; Nayak, M.; Mohanta, S.; Low, J. N.; Ferguson, G.; Glidewell, C., Hydrated hexacyanometallate(III) salts of triaqua(18-crown-6)lanthanoid(III) and tetraaqua(18-crown-6)lanthanoid(III) cations containing nine- and ten-coordinate lanthanoids. *Acta Crystallogr. Sect. C Cryst. Struct. Commun.* **2007**, *63*, m440-m444.

43. Moret, E.; Nicolò, F.; Plancherel, D.; Froidevaux, P.; Bünzli, J.-C. G.; Chapuis, G., Structural and Luminescence Study of the 3:2 Complex between Europium Nitrate and the B Isomer of Dicyclohexyl-18-crown-6. *Helv. Chim. Acta* **1991**, *74*, 65-78.

44. Nicolò, F.; Bünzli, J. C. G.; Chapuis, G., Structure of the 4:3 complex between gadolinium nitrate and 18-crown-6 ether: [Gd(NO$_3$)$_2$(C$_{12}$H$_{24}$O$_6$)]$_3$[Gd(NO$_3$)$_6$]. *Acta Crystallogr. Sect. C Cryst. Struct. Commun.* **1988**, *44*, 1733-1738.

45. Nicolò, F.; Plancherel, D.; Bünzli, J.-C. G.; Chapuis, G., Synthesis, crystal and molecular structure of the 3:2 complex between europium nitrate and theA-isomer of dicyclohexyln-18-crown-6: Conformational study of the ligand. *Helv. Chim. Acta* **1987**, *70*, 1798-1806.

46. Nieland, A.; Mix, A.; Neumann, B.; Stammler, H.-G.; Mitzel, N. W., Cationic rare-earth-metal methyl complexes: a new preparative access exemplified for Y and Pr. *Dalton Trans.* **2010**, *39*, 6753-6753.

47. Nieland, A.; Mix, A.; Neumann, B.; Stammler, H.-G.; Mitzel, N. W., Dicationic Methyl Complexes of the Rare-Earth Elements. *Z.Naturforsch. B* **2014**, *69*, 327-331.

48. Rogers, R. D.; Kurihara, L. K., F-Element/crown ether complexes. 4. Synthesis and crystal and molecular structures of [MCl(OH$_2$)$_2$(18-crown-6)]Cl$_2$.2H$_2$O (M = samarium, gadolinium, terbium). *Inorg. Chem.* **1987**, *26*, 1498-1502.

49. Rogers, R. D.; Rollins, A. N., Primary to secondary sphere coordination of 18-crown-6 to lanthanide (III) nitrates: Structural analysis of [Pr(NO3)3-(18-crown-6)] and [M(NO$_3$)$_3$(OH$_2$)$_3$]·18-crown-6 (M=Y, Eu, Tb−Lu). *J. Chem. Crystallogr.* **1994**, *24*, 321-329.

50. Rogers, R. D.; Rollins, A. N., Mixed anion lanthanide(III) crown ether complexes: crystal structures of [LaCl$_2$(NO$_3$)(12-crown-4)]$_2$, [La(NO$_3$)(OH$_2$)$_4$-(12-crown-4)]Cl$_2$·CH$_3$CN and [LaCl$_2$(NO$_3$)(18-crown-6)]. *Inorg. Chim. Acta* **1995**, *230*, 177-183.

51. Rogers, R. D.; Rollins, A. N.; Etzenhouser, R. D.; Voss, E. J.; Bauer, C. B., Structural investigation into the steric control of polyether complexation in the lanthanide series: macrocyclic 18-crown-6 versus acyclic pentaethylene glycol. *Inorg. Chem.* **1993**, *32*, 3451-3462.

52. Rogers, R. D.; Rollins, A. N.; Henry, R. F.; Murdoch, J. S.; Etzenhouser, R. D.; Huggins, S. E.; Nunez, L., Direct comparison of the preparation and structural features of crown ether and polyethylene glycol complexes of neodymium trichloride hexahydrate. *Inorg. Chem.* **1991**, *30*, 4946-4954.

53. Saleh, M. I.; Kusrini, E.; Fun, H. K.; Yamin, B. M., Structural and selectivity of 18-crown-6 ligand in lanthanide–picrate complexes. *J. Organomet. Chem.* **2008,** *693*, 2561-2571.

54. Starynowicz, P., Europium(II) complexes with unsubstituted crown ethers. *Polyhedron* **2003**, *22*, 337-345.

55. Starynowicz, P., Two complexes of Sm(II) with crown ethers—electrochemical synthesis, structure and spectroscopy. *Dalton Trans.* **2004**, 825-832.

56. Wada, H.; Ooka, S.; Yamamura, T.; Kajiwara, T., Light Lanthanide Complexes with Crown Ether and Its Aza Derivative Which Show Slow Magnetic Relaxation Behaviors. *Inorg. Chem.* **2016**, *56*, 147-155.

57. Yin, H.; Robinson, J. R.; Carroll, P. J.; Walsh, P. J.; Schelter, E. J., κ2-Coordination of 18-crown-6 to Ce(III) cations: solution dynamics and reactivity. *Chem. Commun.* **2014**, *50*, 3470-3470.

58. Yuguo, F.; Cheng, S.; Fengshan, W.; Zhongsheng, J.; Yuan, G.; Jiazan, N., *Fenz.Kex.Yu Huax.Yanjiu* **1984**, *4*, 371-371

59. Yuguo, F.; Jingsheng, Y.; Pinzhe, L.; Zhongsheng, J.; Fenglan, Y.; Shugong, Z.; Jiazuan, N.,. *Yingyong Huaxue(Chin.)(Chin. J. Appl. Chem.)* **1986**, *3*, 35-4.

60. Zhang, S.-Y.; Li, J.; Zeng, Y.; Wen, H.-R.; Du, Z.-Y., Hydrogen-bond-directed assemblies of [La(18-crown-6)(H₂O)₄](BiCl₆)·3H₂O and [Nd(18-crown-6)(H₂O)4](BiCl₆)·3.5H₂O regulated by different symmetries. *J. Mol. Struct.* **2016**, *1125*, 227-233.

61. Wada, H.; Ooka, S.; Yamamura, T.; Kajiwara, T., Light Lanthanide Complexes with Crown Ether and Its Aza Derivative Which Show Slow Magnetic Relaxation Behaviors. *Inorg. Chem.* **2017**, *56*, 147-155.

62. Petrosyants, S.; Dobrokhotova, Z.; Ilyukhin, A.; Efimov, N.; Mikhlina, Y.; Novotortsev, V., Europium and terbium thiocyanates: Syntheses, crystal structures, luminescence and magnetic properties. *Inorg. Chim. Acta* **2015**, *434*, 41-50.

63. Ding, Y.-S.; Han, T.; Hu, Y.-Q.; Xu, M.; Yang, S.; Zheng, Y.-Z., Syntheses, structures and magnetic properties of a series of mono- and di-nuclear dysprosium(iii)-crown-ether complexes: effects of a weak ligand-field and flexible cyclic coordination modes. *Inorg. Chem. Front.* **2016**, *3*, 798-807.

64. Al Hareri, M.; Ras Ali, Z.; Regier, J.; Gavey, E. L.; Carlos, L. D.; Ferreira, R. A. S.; Pilkington, M., Dual-Property Supramolecular H-Bonded 15-Crown-5 Ln(III) Chains: Joint Magneto-Luminescence and *ab Initio* Studies. *Inorg. Chem.* **2017**, *56*, 7344-7353.

65. Gavey, E. L.; Al Hareri, M.; Regier, J.; Carlos, L. D.; Ferreira, R. A. S.; Razavi, F. S.; Rawson, J. M.; Pilkington, M., Placing a crown on Dyɪɪɪ a dual property Lnɪɪɪ crown ether complex displaying optical properties and SMM behaviour. *J. Mater. Chem. C* **2015**, *3*, 7738-7747.

66. Rinehart, J. D.; Long, J. R., Exploiting single-ion anisotropy in the design of f-element single-molecule magnets. *Chem. Sci.* **2011**, *2*, 2078-2085.

67. Chilton, N. F.; Collison, D.; McInnes, E. J. L.; Winpenny, R. E. P.; Soncini, A., An electrostatic model for the determination of magnetic anisotropy in dysprosium complexes. *Nat. Commun.* **2013**, *4*, 2551.

68. Aravena, D.; Ruiz, E., Shedding Light on the Single-Molecule Magnet Behavior of Mononuclear DyIII Complexes. *Inorg. Chem.* **2013**, *52*, 13770-13778.

69. Roos, B. O.; Taylor, P. R.; Siegbahn, P. E. M., A complete active space SCF method (CASSCF) using a density matrix formulated super-CI approach. *Chem. Phys.* **1980**, *48*, 157-173.

70. Blagg, R. J.; Ungur, L.; Tuna, F.; Speak, J.; Comar, P.; Collison, D.; Wernsdorfer, W.; McInnes, E. J. L.; Chibotaru, L. F.; Winpenny, R. E. P., Magnetic relaxation pathways in lanthanide single-molecule magnets. *Nat. Chem.* **2013**, *5*, 673-678.

71. Chibotaru, L. F.; Ungur, L., Ab initio calculation of anisotropic magnetic properties of complexes. I. Unique definition of pseudospin Hamiltonians and their derivation. *J. Chem. Phys.* **2012**, *137*, 064112.

72. Ungur, L.; Chibotaru, L. F., Magnetic anisotropy in the excited states of low symmetry lanthanide complexes. *Phys. Chem. Chem. Phys.* **2011**, *13*, 20086-90.

73. Habib, F.; Luca, O. R.; Vieru, V.; Shiddiq, M.; Korobkov, I.; Gorelsky, S. I.; Takase, M. K.; Chibotaru, L. F.; Hill, S.; Crabtree, R. H.; Murugesu, M., Influence of the Ligand Field on Slow Magnetization Relaxation versus Spin Crossover in Mononuclear Cobalt Complexes. *Angew. Chem. Int. Ed.* **2013**, *52*, 11290-11293.

74. Haenninen, M. M.; Mota, A. J.; Aravena, D.; Ruiz, E.; Sillanpaeae, R.; Camon, A.; Evangelisti, M.; Colacio, E., Two C3-Symmetric Dy$_3$III Complexes with Triple Di-μ-methoxo-μ-phenoxo Bridges, Magnetic Ground State, and Single-Molecule Magnetic Behavior. *Chem. Eur. J.* **2014**, *20*, 8410-8420.

75. Jimenez, J.-R.; Diaz-Ortega, I. F.; Ruiz, E.; Aravena, D.; Pope, S. J. A.; Colacio, E.; Herrera, J. M., Lanthanide Tetrazolate Complexes Combining Single-Molecule Magnet and Luminescence Properties: The Effect of the Replacement of Tetrazolate N3 by β-Diketonate Ligands on the Anisotropy Energy Barrier. *Chem. Eur. J.* **2016**, *22*, 14548-14559.

76. Ruiz, J.; Mota, A. J.; Rodriguez-Dieguez, A.; Titos, S.; Herrera, J. M.; Ruiz, E.; Cremades, E.; Costes, J. P.; Colacio, E., Field and dilution effects on the slow relaxation of a luminescent DyO$_9$ low-symmetry single-ion magnet. *Chem. Commun.* **2012**, *48*, 7916-7918.

77. Wang, L.-F.; Qiu, J.-Z.; Hong, J.-Y.; Chen, Y.-C.; Li, Q.-W.; Jia, J.-H.; Jover, J.; Ruiz, E.; Liu, J.-L.; Tong, M.-L., Tunable Magnetization Dynamics through Solid-State Ligand Substitution Reaction. *Inorg. Chem.* **2017**, *56*, 8829-8836.

78. Wang, L.-F.; Qiu, J.-Z.; Liu, J.-L.; Chen, Y.-C.; Jia, J.-H.; Jover, J.; Ruiz, E.; Tong, M.-L., Modulation of single-molecule magnet behaviour via photochemical [2+2] cycloaddition. *Chem. Commun.* **2015**, *51*, 15358-15361.

79. Atanasov, M.; Zadrozny, J. M.; Long, J. R.; Neese, F., A theoretical analysis of chemical bonding, vibronic coupling, and magnetic anisotropy in linear iron(ii) complexes with single-molecule magnet behavior. *Chem. Sci.* **2013**, *4*, 139-156.

80. Malmqvist, P. Å.; Roos, B. O.; Schimmelpfennig, B., The restricted active space (RAS) state interaction approach with spin-orbit coupling. *Chem. Phys. Lett.* **2002**, *357*, 230-240.

81. Roos, B. O.; Lindh, R.; Malmqvist, P.-A.; Veryazov, V.; Widmark, P.-O.; Borin, A. C., New relativistic atomic natural orbital basis sets for lanthanide atoms with applications to the Ce diatom and LuF3. *J. Phys. Chem. A* **2008**, *112*, 11431-11435.

82. Roos, B. O.; Lindh, R.; Malmqvist, P. Å.; Veryazov, V.; Widmark, P. O., Main Group Atoms and Dimers Studied with a New Relativistic ANO Basis Set. *J. Phys. Chem. A* **2004**, *108*, 2851-2858.

83. Widmark, P.-O.; Malmqvist, P.-k.; Roos, B. r. O., Density matrix averaged atomic natural orbital (ANO) basis sets for correlated molecular wave functions. *Theor. Chim. Acta* **1990**, *77*, 291-306.

84. Aquilante, F.; Autschbach, J.; Carlson, R. K.; Chibotaru, L. F.; Delcey, M. G.; De Vico, L.; Fdez. Galván, I.; Ferré, N.; Frutos, L. M.; Gagliardi, L.; Garavelli, M.; Giussani, A.; Hoyer, C. E.; Li Manni, G.; Lischka, H.; Ma, D.; Malmqvist, P. Å.; Müller, T.; Nenov, A.; Olivucci, M.; Pedersen, T. B.; Peng, D.; Plasser, F.; Pritchard, B.; Reiher, M.; Rivalta, I.; Schapiro, I.; Segarra-Martí, J.; Stenrup, M.; Truhlar, D. G.; Ungur, L.; Valentini, A.; Vancoillie, S.; Veryazov, V.; Vysotskiy, V. P.; Weingart, O.; Zapata, F.; Lindh, R., Molcas 8: New capabilities for multiconfigurational quantum chemical calculations across the periodic table. *J. Comput. Chem.* **2016**, *37*, 506-54.1

85. Ungur, L.; Chibotaru, L. Strategies toward High-Temperature Lanthanide-based Single-molecule Magnets. *Inorg. Chem.* **2016**, *556*, 10043-10056.

86. Becke, A. D., Density-functional thermochemistry. III. The role of exact exchange. *J. Chem. Phys.* **1993**, *98*, 5648-5652.

87. Schäfer, A.; Huber, C.; Ahlrichs, R., Fully optimized contracted Gaussian basis sets of triple zeta valence quality for atoms Li to Kr. *J. Chem. Phys.* **1994**, *100*, 5829-5835.

88. Frisch, M. J.; Trucks, G. W.; Schlegel, H. B.; Scuseria, G. E.; Robb, M. A.; Cheeseman, J. R.; Scalmani, G.; Barone, V.; Mennucci, B.; Petersson, G. A.; Nakatsuji, H.; Caricato, M.; Li, X.; Hratchian, H. P.; Izmaylov, A. F.; Bloino, J.; Zheng, G.; Sonnenberg, J. L.; Hada, M.; Ehara, M.; Toyota, K.; Fukuda, R.; Hasegawa, J.; Ishida, M.; Nakajima, T.; Honda, Y.; Kitao, O.; Nakai, H.; Vreven, T.; Montgomery J. A, Jr.; Peralta, J. E.; Ogliaro, F.; Bearpark,

M.; Heyd, J. J.; Brothers, E.; Kudin, K. N.; Staroverov, V. N.; Kobayashi, R.; Normand, J.; Raghavachari, K.; Rendell, A.; Burant, J. C.; Iyengar, S. S.; Tomasi, J.; Cossi, M.; Rega, N.; Millam, N. J.; Klene, M.; Knox, J. E.; Cross, J. B.; Bakken, V.; Adamo, C.; Jaramillo, J.; Gomperts, R.; Stratmann, R. E.; Yazyev, O.; Austin, A. J.; Cammi, R.; Pomelli, C.; Ochterski, J. W.; Martin, R. L.; Morokuma, K.; Zakrzewski, V. G.; Voth, G. A.; Salvador, P.; Dannenberg, J. J.; Dapprich, S.; Daniels, A. D.; Farkas, Ö.; Foresman, J. B.; Ortiz, J. V.; Cioslowski, J.; Fox, D. J. *Gaussian 09 (Revision A.1)*, Wallingford, CT, 2009.

89. Aravena, D. Ab Initio Prediction of Tunneling Relaxation Times and Effective Demagnetication Barriers in Kramers Lanthanide Single-Molecule Magnets. *J. Phys. Chem. Lett.* **2018**, *9*, 5327-5333.

90 Llunell, M.; Casanova, D.; Cirera, J.; Alemany, P.; Alvarez, S. *Shape (version 2.1)*, Universitat de Barcelona: 2013.

91. Ding, Y.-S.; Yu, K.-X.; Reta, D.; Ortu, F.; Winpenny, R. E. P.; Zheng, Y.-Z.; Chilton, N. F. Final- and temperature-dependent quantum tunnelling of the magnetisation in a large barrier single-molecule magnet. *Nat. Commun.* **2018**, 9, 3134.

92. Liddle, S. T.; van Slageren, J. Improving f-elements single molecule magnets. *Chem. Soc. Rev.* **2015**, *44*, 6655-6669.

For Table of Contents only

Synthesis and structural and magnetic characterization of $[Ln(H_2O)_3(18\text{-crown-}6)](ClO_4)_3$ (Ln: Tb_{III}, Dy_{III}, Er_{III} and Yb_{III}) has been performed. Ab initio CASSCF-type calculations were carried out to understand the existence of slow spin relaxation under an external magnetic field only in Dy_{III} and Yb_{III} compounds. The analysis of the spin relaxation times reveals that quantum tunneling and Raman relaxation are predominant.